# A ring of eight conserved negatively charged amino acids doubles the conductance of BK channels and prevents inward rectification

**Tinatin I. Brelidze, Xiaowei Niu, and Karl L. Magleby***

Department of Physiology and Biophysics, University of Miami School of Medicine, 1600 N.W. 10th Avenue, Miami, FL 33136

Edited by Charles F. Stevens, The Salk Institute for Biological Studies, La Jolla, CA, and approved May 30, 2003 (received for review April 16, 2003)

**Large-conductance $Ca^{2+}$–voltage-activated $K^+$ channels (BK channels) control many key physiological processes, such as neurotransmitter release and muscle contraction. A signature feature of BK channels is that they have the largest single channel conductance of all $K^+$ channels. Here we examine the mechanism of this large conductance. Comparison of the sequence of BK channels to lower-conductance $K^+$ channels and to a crystallized bacterial $K^+$ channel (MthK) revealed that BK channels have a ring of eight negatively charged glutamate residues at the entrance to the intracellular vestibule. This ring of charge, which is absent in lower-conductance $K^+$ channels, is shown to double the conductance of BK channels for outward currents by increasing the concentration of $K^+$ in the vestibule through an electrostatic mechanism. Removing the ring of charge converts BK channels to inwardly rectifying channels. Thus, a simple electrostatic mechanism contributes to the large conductance of BK channels.**

Large-conductance $Ca^{2+}$–voltage-activated $K^+$ (BK) channels are activated in a highly synergistic manner by intracellular $Ca^{2+}$ ($Ca_i^{2+}$) and membrane depolarization (1–9). When open, the efflux of $K^+$ out of the cell hyperpolarizes the membrane potential, turning off voltage-dependent $Ca^{2+}$ channels and reducing the influx of $Ca^{2+}$ available to both activate BK channels and control cellular processes. This negative feedback mechanism allows BK channels to play a key role in regulating many physiological processes, such as neurotransmitter release (10, 11), repetitive firing of neurons (12), spike broadening during repetitive firing (13), the electrical tuning of hair cells in the cochlea (14, 15), and muscle contraction (16).

BK channels (for big $K^+$) have the largest single-channel conductance of all $K^+$ selective channels, being 250–300 pS in symmetrical 150 mM KCl (8, 17–20). Like most $K^+$ channels of lower conductance, BK channels have a tetrameric structure, with four $\alpha$ subunits forming functional channels. BK channels also have the same selectivity filter sequence (GYG) found in most other $K^+$ channels of lower conductance (21). Thus, the question arises as to why the conductance of BK channels is so big.

Previous experimental and theoretical work has suggested that charged residues located in the vestibules and pores of ion channels can play a major role in controlling the unitary conductance through an electrostatic mechanism (22–30). Such rings of fixed charge could increase the concentration of the permeating ions in the vestibules of the channels, leading to increased availability of ions to transit the selectivity filter, which would increase the unitary (single-channel) conductance.

In this study we show by comparison of the sequence of BK channels to lower-conductance $K^+$ channels and to a bacterial $K^+$ channel (MthK) crystallized in the open state (31) that BK channels have a ring of eight negatively charged glutamate residues at the entrance to the intracellular vestibule that are missing in lower-conductance $K^+$ channels. We find that the single-channel conductance decreases progressively as the net charge in the ring of charge is changed from $-8$ to $+8$. This effect of charge on conductance is abolished at high intracellular $K^+$ ($K_i^+$), indicating that the ring of charge increases conductance by concentrating $K^+$ in the vestibule through an electrostatic mechanism. The concentration of $K^+$ in the vestibule by the ring of charge is found to be equivalent to that achieved by increasing the $K^+$ in the bulk intracellular solution from 150 to 500 mM. This simple electrostatic mechanism was found to double the conductance of BK channels for outward currents, which is the direction of $K^+$ current for physiological conditions.

We observe that outward and inward single-channel current amplitudes through BK channels are symmetrical in symmetrical 150 mM KCl solution over the examined range of voltage, from $-250$ mV to $+250$ mV. The ring of charge is found to have little effect on inward currents, while doubling the outward single-channel currents. Thus, without the ring of charge, BK channels become inwardly rectifying channels.

## Materials and Methods

**Expression and Mutagenesis.** The construct encoding the WT BK channel used in these experiments (mSlo1 in pcDNA3) was kindly provided by Merck. This construct was initially cloned by Pallanck and Ganetzky (32) (GenInfo Identifier no. 487796) and then modified by Merck (33) to remove all 5′ noncoding sequence up to the second potential initiation site (1–940 was removed). The cRNA was transcribed by using the mMessage mMachine kit (Ambion, Austin, TX) and injected in *Xenopus laevis* oocytes at ≈0.5–2 ng per oocyte, 2–8 days before recording (34). Mutagenesis was carried out by using the Quick-Change XL site-directed mutagenesis kit (Stratagene) and checked by sequencing.

**Single-Channel Recordings and Analysis.** Single-channel currents were recorded from BK channels expressed in oocytes by using the inside-out configuration of the patch-clamp technique (35). Data were acquired with an Axopatch 200A amplifier (Axon Instruments, Foster City, CA), sampled every 3 $\mu$s by using a Digidata 1200A (Axon Instruments) and PCLAMP7, and further analyzed with custom software. The voltage/current relationship of the Axopatch 200A was found to be linear over the examined range of $-400$ mV to $+400$ mV, as determined with a model cell. The effective filtering ranged from 5 to 15 kHz and had no effect on the measured conductance over this range because the open and closed current levels were well defined. Patches with one to three BK channels were used for analysis. BK channels were identified from their characteristic voltage and $Ca^{2+}$ sensitivity (1). Single-channel current amplitudes were measured in an unbiased manner by using all-point histograms of the current records, with the single-channel current amplitudes indicated by the distance between the peaks of the histograms. For patches with multiple channels, the single-channel current amplitude for

This paper was submitted directly (Track II) to the PNAS office.

Abbreviations: BK channel, large-conductance $Ca^{2+}$– voltage-activated $K^+$ channel; $Ca_i^{2+}$, intracellular $Ca^{2+}$; $K_i^+$, intracellular $K^+$.

*To whom correspondence should be addressed. E-mail: kmagleby@miami.edu.

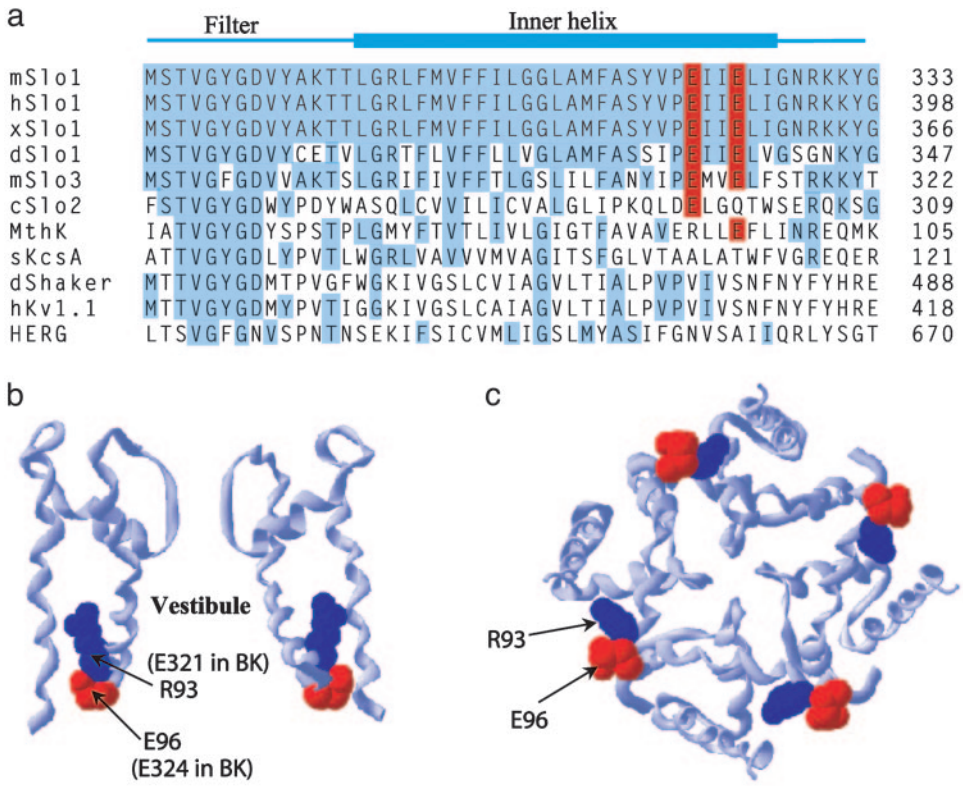


**Fig. 1.** Eight conserved negatively charged glutamate residues ring the entrance to the intracellular vestibule of BK channels, but not the vestibule of low-conductance $K^+$ channels. (*a*) Sequence alignment to GYG of the indicated $K^+$ channels for the selectivity filter and inner helix region. Blue indicates residues identical to mouse BK channels (mSlo1), except that E321 and E324 that form the ring of charge are in red. The GenInfo Identifier nos. are: mSlo1, 487797; hSlo1, 26638650; xSlo1, 14582152; dSlo1, 321029; mSlo3, 6680542; cSlo2, 7188777; MthK, 2622639; sKcsA, 2127577; dShaker, 85110; hKv1.1, 1168947; HERG, 7531135. (*b* and *c*) Ribbon representation of the crystal structure of the MthK channel obtained with Swiss Protein Viewer from the atomic coordinates by Jiang *et al.* (31). The residues R93 and E96 in MthK that correspond to E321 and E324 in BK channels are presented as space-filling surfaces. A side view with only two subunits is presented (*b*), and a view down the pore of the channel from the intracellular side with all four subunits is presented (*c*).

that patch was given by the average for the channels in the patch. Each of the plotted points in the figures represent the average of observations obtained from three or more patches, with the SE of the observations indicated by the error bars. The absence of visible error bars indicates that the SE is less than the symbol size. Experiments were performed at 21–23°C.

Unless indicated, the extracellular (pipette) and intracellular solutions contained 150 mM KCl, 1 mM EGTA, and 1 mM *N*-tris[hydroxymethyl]methyl-2-aminoethane-sulfonic acid (HEDTA) to bind $Ca^{2+}$ to prevent possible $Ca^{2+}$ block from contaminating $Ca^{2+}$, and 5 mM *N*-(2-hydroxyethyl)-ethylenediamine-*N*,*N*′,*N*′-triacetic acid (TES) to buffer the pH (adjusted to pH 7.0). The intracellular solution also typically contained 50 $\mu$M crown ether (+)-(18-crown-6)-2,3,11,12-tetra-carboxylic acid to bind $Ba^{2+}$ to prevent $Ba^{2+}$ block of the channel (36). $GdCl_3$ (60 $\mu$M) was typically added to pipette solutions to block endogenous mechanosensitive channels (37). The intracellular $K^+$ was varied as indicated by changing the concentration of KCl. Solutions were changed with a micro chamber as described (1). For the mutation E321D, $Ca^{2+}$ was added to bring free $Ca_i^{2+}$ to 0.1 mM for the lower voltages from +30 to +80 mV to facilitate activation of the channel. This level of $Ca^{2+}$ at these voltages has little effect on conductance (38). In experiments using large negative membrane potentials to obtain inward currents, free $Ca_i^{2+}$ was 0.1–1 mM $Ca_i^{2+}$ to activate the channel. Free $Ca_i^{2+} \leq 1$ mM has little effect on inward current amplitudes (38). As expected from the laws of thermodynamics (17), changing the net charge in the ring of charge did not change the reversal potential.

## Results

**BK Channels Have a Ring of Eight Negative Charges.** If the large conductance of BK channels arises from charged residues, then BK channels should have negatively charged residues associated with the conduction pathway that would be absent in $K^+$ channels of lower conductance. Because BK channels are tetramers formed from four $\alpha$ subunits (39), any charged residues in the primary sequence would be present in all four subunits, forming a ring of charge around the pore of the channel.

To look for such a ring of charge, we compared the sequence of BK channels to the sequence of other $K^+$ channels (Fig. 1*a*), with the alignment made to the selectivity filter signature sequence (GYG or GFG). BK channels from nine different species were examined (mouse, human, frog, fly, dog, cow, chicken, cockroach, and *Caenorhabditis elegans*), and all had conserved negative residues at positions equivalent to 321 and 324 in the mouse BK channel (mSlo1). Alignments from mouse, human (hSlo1), frog (xSlo), and fly (dSlo1) BK channels are presented in Fig. 1*a*. Two BK-like channels with somewhat smaller conductance than BK channels (100–200 pS) had either two conserved negative charges (mSlo3) (40, 41) or one conserved negative charge (cSlo2) (42). MthK, a bacterial $Ca^{2+}$-regulated $K^+$ channel (31) with conductance of $\approx$100 pS at +25 mV has two negative charges and one positive charge in the region equivalent to 321 and 324 of BK channels. The other listed $K^+$ channels (KcsA, Shaker, Kv1.1, and HERG) do not have charged residues in this region, and all have considerably smaller unitary conductance (<50 pS). The alignments in Fig. 1*a* suggest

that the conserved glutamate residues E321 and E324 may be a contributing factor in the large unitary conductance of BK channels.

**Eight Negatively Charged Residues Ring the Intracellular Vestibule.** To obtain an estimate of where these negatively charged glutamate residues might be located in relationship to the conduction pathway of BK channels, we assumed that the general structures of the inner vestibule of BK and MthK channels are similar. Using the atomic coordinates for MthK (31), we generated the ribbon structure of MthK for two opposite subunits, as viewed from the side with the intracellular surface down (Fig. 1*b*), and for all four subunits, as viewed from the intracellular side of the membrane looking into the vestibule (Fig. 1*c*). From the alignment in Fig. 1*a* it can be seen that E321 and E324 in BK would correspond to R93 and E96 in MthK, respectively. Thus, assuming BK channels have a structure similar to MthK, the relative positions of E321 and E324 in BK channels would be given by the blue (R93) and red (E96) residues, respectively, in MthK (Fig. 1 *b* and *c*). On this basis, the conserved negative residues E321 and E324 in BK channels would be located at the entrance to the intracellular vestibule, with E321 about one turn of the $\alpha$-helix deeper in the vestibule than E324. Although the exact location of E321 and E324 in BK channels may differ from that shown in Fig. 1 *b* and *c* for MthK, such a comparison does suggest that these charged residues are near the entrance to the intracellular vestibule in BK channels. By providing two negative residues for each of the four subunits in BK channels, E321 and E324 would then form a ring of eight negative charges at the entrance to the intracellular vestibule of BK channels.

**Single-Channel Conductance Depends on the Net Charge in the Ring of Charge.** If the ring of negative charge increases the single-channel conductance of BK channels by increasing the concentration of $K^+$ in the vestibule, then decreasing the negative charge in the ring of charge should decrease the conductance. To explore this possibility, we measured single-channel currents over a range of voltage with different amounts of charge in the ring of charge. As the net charge in the ring of charge was changed from $-8$ in WT BK channels to $-4$ with either of the mutations E321N or E324N, to 0 with E321N/E324N, and to $+8$ with E321K/E324K, the single-channel current amplitudes progressively decreased (Fig. 2*a*, 150 mM $K_i^+$). This pronounced effect of charge on single-channel conductance was observed for outward currents over a wide range of voltage (Fig. 2*b*). The two different mutations (E321N or E324N) used to remove four negative charges reduced the single-channel currents an equal amount, suggesting that these sites are equivalent in their effects on the current.

In addition to the effects of the net charge in the ring of charge on single-channel conductance, changes in the net charge typically changed the gating and open probability, depending on the mutations. These changes in gating have not been examined for this article, which is concerned with single-channel conductance.

**The Ring of Eight Negative Charges Concentrates $K^+$ in the Intracellular Vestibule Through an Electrostatic Mechanism.** The results in Fig. 2 *a* and *b* show that the ring of negative charge greatly increased the outward single-channel currents through BK channels when the $K_i^+$ was 150 mM. If this increase arises because the ring of charge increases the concentration of $K^+$ in the vestibule through an electrostatic mechanism, then the effect of the ring of charge on increasing current should be greatest at low $K_i^+$, becoming insignificant at very high $K_i^+$ (28, 30, 43, 44). To test this possibility we obtained single-channel currents with 500 mM and 3.4 M $K_i^+$ for comparison to those obtained with 150 mM $K_i^+$. Increasing $K_i^+$ increased the magnitude of the single-channel currents while decreasing the effect of the ring of charge (Fig. 2*a*). This decreased effect of charge at high $K_i^+$ was observed over a range of voltages (Fig. 2 *b–d*). The effect of net charge on the single-channel conductance over a range of $K_i^+$ is summarized in Fig. 2*e*. Consistent with an electrostatic mechanism, the ring of charge had its greatest effect at low $K_i^+$ (150 mM $KCl_i$), less of an effect at intermediate $K_i^+$ (500 mM $KCl_i$), and negligible effect at very high $K_i^+$ (3.4 M $KCl_i$). At low $K_i^+$, the extra $K^+$ ions attracted to the vestibule by the ring of charge would lead to significant increases in the concentration of $K^+$ in the vestibule when compared with the concentration of $K^+$ in the intracellular solution, whereas at very high $K_i^+$, the extra $K^+$ attracted by the ring of charge would be insignificant compared with the high $K^+$ already present.

**The Ring of Charge Has Little Effect on the Inward Currents.** Although our results are consistent with an electrostatic mechanism, it is possible that changing the net charge in the ring of charge might act by physically altering the structure of the conduction pathway to change the resistance to the passage of $K^+$ ions, rather than by concentrating $K^+$ in the intracellular vestibule. If changes in the net charge act indirectly to partially close the vestibule or perhaps induce changes in the structure of the selectivity filter, then changing the net charge in the ring of charge might be expected to alter both inward currents and outward currents. Supporting an electrostatic rather than structural mechanism, the net charge in the ring of charge had little effect on inward currents (Fig. 3 *a* and *b*).

**Further Support for an Electrostatic Mechanism.** Also consistent with an electrostatic rather than a structural mechanism, the reduction in single-channel current amplitudes was the same for the E321N and E324N mutations, both of which gave a net charge of $-4$, for mutations at different sites (Fig. 2). As an additional test of the electrostatic mechanism, we maintained the net charge at $-8$ with the mutation E321D and found no effect on the single-channel current amplitudes (Fig. 3*c*) over a range of voltage [Fig. 2*b*, compare WT (•) to E321D (○)]. The observations in this section suggest, then, that the single-channel current amplitude depends on the net charge rather than the specific residue or minor differences in location.

**Estimating the Increase in the Effective $K^+$ in the Intracellular Vestibule Induced by the Ring of Charge.** The experiments described above suggest that the ring of eight negative charges located at the entrance to the intracellular vestibule of BK channels increases single-channel conductance by concentrating $K^+$ in the vestibule. We estimated the effective increase in concentration by determining what concentration of $K^+$ in the intracellular solution in the absence of the ring of charge would be required to give the same single-channel current amplitude as in the presence of the ring of charge. With 150 mM $K_i^+$ at $+100$ mV, the single channel currents were 30 pA for WT channels (Fig. 4*a Left*). Removing the ring of charge with the mutation E321N/E324N then reduced the single-channel current amplitudes to 15 pA (Fig. 4*a Center*). Increasing $K_i^+$ to 500 mM then restored the currents to 30 pA (Fig. 4*a Right*). Similar measurements over a range of voltage indicated that increasing $K_i^+$ from 150 to 500 mM restored the single-channel current amplitude in channels with no net charge in the ring of charge to the same level as currents in WT channels with eight negative charges in the ring of charge (Fig. 4*b*). Thus, with 150 mM $K_i^+$, eight negative charges at the entrance to the vestibule increase the effective concentration of $K^+$ in the vestibule the same amount that increasing $K_i^+$ from 150 to 500 mM would in the absence of charge.

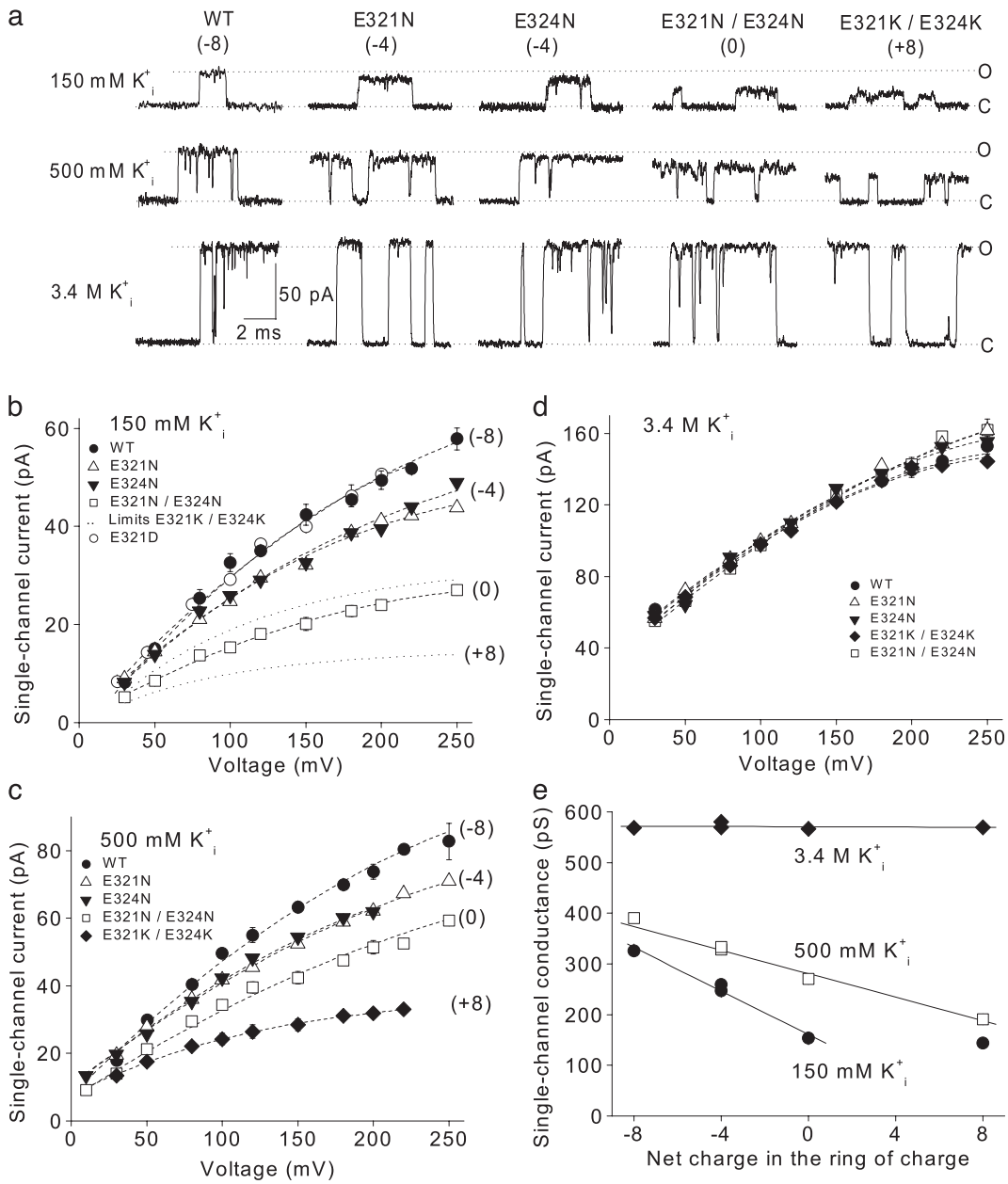


**Fig. 2.** The ring of eight negative charges at the intracellular vestibule doubles the single-channel conductance of BK channels by an electrostatic mechanism. (*a*) Representative single-channel current records for WT and four different mutant channels at the indicated $K_i^+$. The net charge on the ring of charge for WT and mutant channels is indicated. Open (O) and closed (C) current levels are indicated. Membrane voltage is +100 mV; $K_o^+$ was 150 mM. The open current levels were well defined for all experiments with WT and the various mutant channels with different amounts of net charge, except for the one experimental condition of +8 charges and 150 mM $K_i^+$, where the open current level was unstable, perhaps because the channel did not lock into a stable open conformation under these conditions. Increasing the $K_i^+$ for channels with +8 charges to either 500 or 3.4 M $K_i^+$ gave stable, well defined open current levels. (*b–d*) Plots of outward single-channel current amplitudes versus voltage for the WT and mutant channels for the indicated $K_i^+$. The net charge in the ring of charge is indicated. The absence of visible error bars indicates the SE is less than the size of the symbol. All plotted points in *b–d* and the lower dotted line in *b* indicate current amplitudes estimated by all-point histograms of the single-channel current. The upper dotted line in *b* indicates the highest current levels that occurred infrequently for +8 charges and 150 mM $K_i^+$. These brief higher current levels were measured by hand, as they had little effect on the current histograms. The open circles in *b* for data from E321D at +30, +50, and +80 mV have been shifted 5 mV to the left so they can be seen. (*e*) Plots of outward single-channel cord conductance at +100 mV versus net charge in the ring of charge at the indicated $K_i^+$. The reversal potentials used to determine cord conductance were calculated from the activities of $K^+$ with the Nernst equation and were 0 mV for 150 $K_i^+$, −27 mV for 500 mM $K_i^+$, and −72 mV for 3.4 M $K_i^+$. $K_o^+$ was 150 mM. For 150 mM $K_i^+$ the line was only fitted from −8 to 0 net charge, with the remaining point at +8 charge and 150 mM $K_i^+$ plotting the average of the levels indicated by the dashed lines in *b*.

**Converting BK Channels to Inwardly Rectifying Channels.** Consistent with little effect of the ring of charge on inward single-channel currents (Fig. 3 *a* and *b*) and a marked reduction of outward single-channel currents in the absence of the ring of charge (Fig. 2), removing the ring of charge converted BK channels into inwardly rectifying channels (Fig. 5).

## Discussion

BK channels have the largest single-channel conductance among all $K^+$ channels. Despite their unusually large conductance, BK channels are highly selective for $K^+$ over $Na^+$ (20, 45, 46), and most likely have pore architecture similar to that of lower-

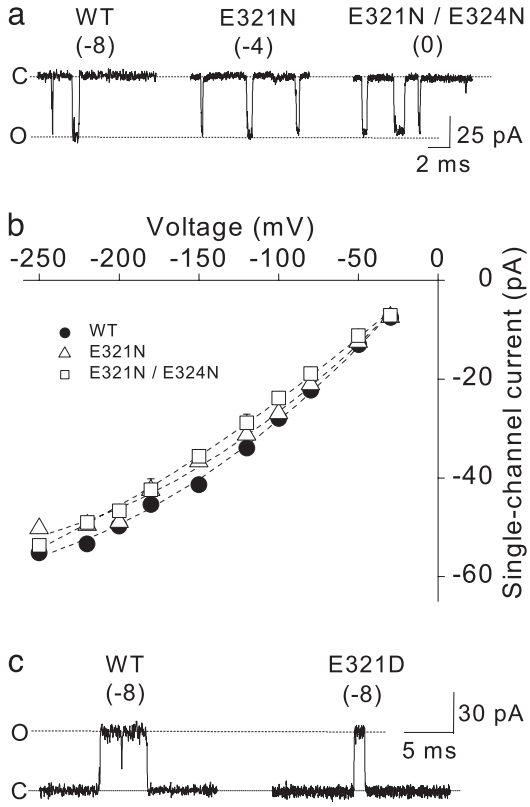


**Fig. 3.** The ring of eight negative charges has little effect on inward single-channel current amplitudes, and the mutation E321D has no effect on outward single-channel current amplitude. (*a*) Representative inward single-channel currents from WT and mutant channels. The net charge on the ring of charge for WT and mutant channels is indicated. Membrane voltage was −200 mV. (*b*) Plots of inward single-channel current amplitude versus voltage. (*c*) Representative outward single-channel currents for the WT and mutant E321D BK channels. Membrane voltage was +150 mV. Symmetrical 150 mM $K^+$ was used in *a*–*c*.

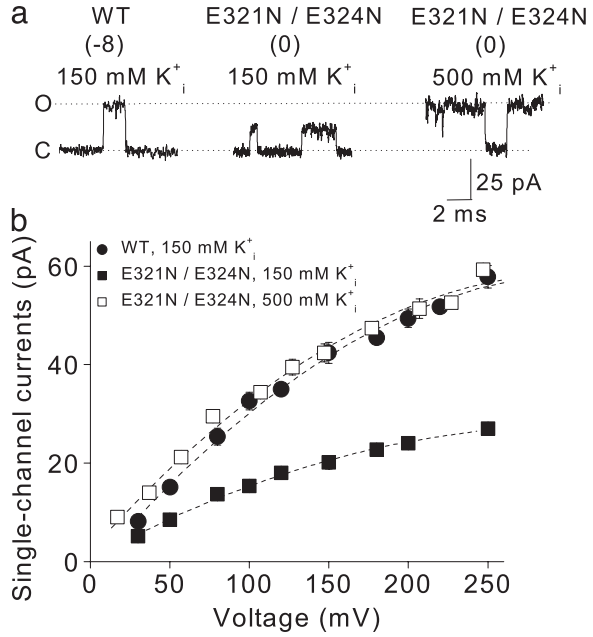


**Fig. 4.** The ring of charge increases the effective concentration of $K^+$ in the intracellular vestibule equivalent to that obtained when the $K_i^+$ is increased from 150 to 500 mM. (*a*) Representative single-channel currents from WT and mutant channels at the indicated $K_i^+$. The net charge on the ring of charge is indicated. Membrane voltage was +100 mV for records with 150 mM $K_i^+$. The voltage was +80 mV for recordings with 500 mM $K_i^+$ to approximately compensate for the greater driving force with 500 mM $K_i^+$. To fully compensate would require a record at +73 mV, but there would be little difference between the records at +73 and +80, as seen in *b*. The $K_o^+$ was 150 mM. (*b*) Plots of single-channel current amplitude versus membrane voltage for the indicated channels. The plotted data points with 500 mM $K_i^+$ were shifted to the right by 27 mV, the absolute magnitude of the calculated shift in reversal potential, to compensate for the greater driving force on $K_i^+$ with 500 mM $K_i^+$.

conductance $K^+$ channels, including a wide inner vestibule and a narrow selectivity filter (31, 47, 48). In this study we show that BK channels double their outward single-channel conductance by using a ring of eight negatively charged residues located at the entrance to the intracellular vestibule. We further show that this doubling in currents results from an electrostatic mechanism, with the ring of negative charge effectively concentrating $K^+$ in the vestibule to provide a ready source of $K^+$ to carry outward current. Doubling the conductance would decrease the number of BK channels required in the cell, and hence reduce the metabolic costs associated with the production of such channels.

With 150 mM $K_i^+$, a volume equivalent to that of an intracellular vestibule with a diameter and depth of 20 Å would contain, on average, only 0.56 molecules of $K^+$. For a single-channel current of 32 pA, one $K^+$ ion would transit the channel to the extracellular side every 5 ns, indicating the minimal rate at which $K^+$ would have to enter the intracellular vestibule. The ring of negative charge would increase the probability of $K^+$ being in the vestibule, and hence, increase the probability that $K^+$ would be available to enter the narrow selectivity filter (see Fig. 1*b*) for transit through the channel.

WT BK channels have linear i/V curves with 150 mM symmetrical KCl for limited ranges of voltage (45). This symmetry in currents occurs even though the expected structure of BK channels would be asymmetrical, with a deep intracellular vestibule and a shallow extracellular vestibule. We found that removing the ring of charge converted BK channels into inwardly rectifying channels (Fig. 5). Thus, the eight negative charges in the ring of charge preserve the symmetry of inward and outward currents with symmetrical 150 mM KCl, by doubling the mag-

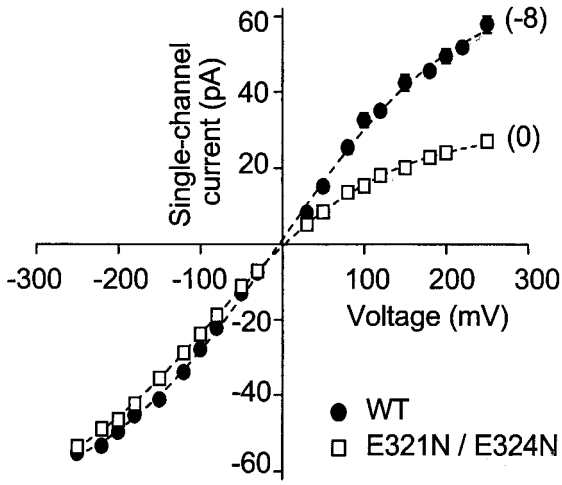


**Fig. 5.** Removing the ring of eight negative charges converts BK channels to inwardly rectifying channels. Plots of single-channel current amplitudes versus membrane voltage for WT channels and a mutant channel with no charge in the ring of charge. The net charge on the ring of charge for the WT and the mutant channel is indicated by each curve. Symmetrical 150 mM $K^+$ was used.

nitude of the outward currents while having little effect on the inward currents. It is the outward current that is important for the physiological function of the channel, because under physiological conditions currents through BK channels are outward.

Unlike the outward currents, the inward currents through BK channels are little affected by the charge in the ring of charge, and even after removing the ring of charge, both the outward and the inward conductances of BK channels are still much larger than for most other $K^+$ channels. Thus, while the ring of charge is a major contributor to the large conductance of BK channels for outward currents, other factors in addition to the ring of charge must also contribute toward the large outward and inward currents. Because of the multiple factors the larger conductance of BK channels most likely evolved in multiple steps. Whether the evolutionary forces were to specifically increase conductance or alter gating is not clear, as our observations peripheral to this study indicated that changes in the charge in the ring of charge also alter the gating kinetics.

This work was supported in part by grants to K.L.M. from the Florida Department of Health Biomedical Research Program and the National Institutes of Health.

1. Barrett, J. N., Magleby, K. L. & Pallotta, B. S. (1982) *J. Physiol.* (*London*) **331,** 211–230.
2. Rothberg, B. S. & Magleby, K. L. (2000) *J. Gen. Physiol.* **116,** 75–99.
3. Rothberg, B. S. & Magleby, K. L. (1999) *J. Gen. Physiol.* **114,** 93–124.
4. Cox, D. H. & Aldrich, R. W. (2000) *J. Gen. Physiol.* **116,** 411–432.
5. Cui, J. & Aldrich, R. W. (2000) *Biochemistry* **39,** 15612–15619.
6. Xia, X. M., Zeng, X. & Lingle, C. J. (2002) *Nature* **418,** 880–884.
7. Magleby, K. L. (2003) *J. Gen. Physiol.* **121,** 81–96.
8. Latorre, R., Oberhauser, A., Labarca, P. & Alvarez, O. (1989) *Annu. Rev. Physiol.* **51,** 385–399.
9. Moczydlowski, E. & Latorre, R. (1983) *J. Gen. Physiol.* **82,** 511–542.
10. Wang, Z. W., Saifee, O., Nonet, M. L. & Salkoff, L. (2001) *Neuron* **32,** 867–881.
11. Robitaille, R., Garcia, M. L., Kaczorowski, G. J. & Charlton, M. P. (1993) *Neuron* **11,** 645–655.
12. Viana, F., Bayliss, D. A. & Berger, A. J. (1993) *J. Neurophysiol.* **69,** 2150–2163.
13. Shao, L. R., Halvorsrud, R., Borg-Graham, L. & Storm, J. F. (1999) *J. Physiol.* (*London*) **521,** 135–146.
14. Fettiplace, R. & Fuchs, P. A. (1999) *Annu. Rev. Physiol.* **61,** 809–834.
15. Rosenblatt, K. P., Sun, Z. P., Heller, S. & Hudspeth, A. J. (1997) *Neuron* **19,** 1061–1075.
16. Brenner, R., Perez, G. J., Bonev, A. D., Eckman, D. M., Kosek, J. C., Wiler, S. W., Patterson, A. J., Nelson, M. T. & Aldrich, R. W. (2000) *Nature* **407,** 870–876.
17. Hille, B. (2001) *Ion Channels of Excitable Membranes* (Sinauer, Sunderland, MA).
18. Marty, A. (1981) *Nature* **291,** 497–500.
19. Pallotta, B. S., Magleby, K. L. & Barrett, J. N. (1981) *Nature* **293,** 471–474.
20. Yellen, G. (1984) *J. Gen. Physiol.* **84,** 157–186.
21. Heginbotham, L., Lu, Z., Abramson, T. & MacKinnon, R. (1994) *Biophys. J.* **66,** 1061–1067.
22. Imoto, K., Busch, C., Sakmann, B., Mishina, M., Konno, T., Nakai, J., Bujo, H., Mori, Y., Fukuda, K. & Numa, S. (1988) *Nature* **335,** 645–648.
23. Smith, S. S., Liu, X., Zhang, Z. R., Sun, F., Kriewall, T. E., McCarty, N. A. & Dawson, D. C. (2001) *J. Gen. Physiol.* **118,** 407–431.
24. Li, R. A., Velez, P., Chiamvimonvat, N., Tomaselli, G. F. & Marban, E. (2000) *J. Gen. Physiol.* **115,** 81–92.
25. Cai, M. & Jordan, P. C. (1990) *Biophys. J.* **57,** 883–891.
26. MacKinnon, R., Latorre, R. & Miller, C. (1989) *Biochemistry* **28,** 8092–8099.
27. MacKinnon, R. & Miller, C. (1989) *Biochemistry* **28,** 8087–8092.
28. Green, W. N. & Andersen, O. S. (1991) *Annu. Rev. Physiol.* **53,** 341–359.
29. Consiglio, J. F., Andalib, P. & Korn, S. J. (2003) *J. Gen. Physiol.* **121,** 111–124.
30. Kienker, P., Tomaselli, G., Jurman, M. & Yellen, G. (1994) *Biophys. J.* **66,** 325–334.
31. Jiang, Y., Lee, A., Chen, J., Cadene, M., Chait, B. T. & MacKinnon, R. (2002) *Nature* **417,** 515–522.
32. Pallanck, L. & Ganetzky, B. (1994) *Hum. Mol. Genet.* **3,** 1239–1243.
33. McManus, O. B., Helms, L. M., Pallanck, L., Ganetzky, B., Swanson, R. & Leonard, R. J. (1995) *Neuron* **14,** 645–650.
34. Qian, X., Nimigean, C. M., Niu, X., Moss, B. L. & Magleby, K. L. (2002) *J. Gen. Physiol.* **120,** 829–843.
35. Hamill, O. P., Marty, A., Neher, E., Sakmann, B. & Sigworth, F. J. (1981) *Pflügers Arch.* **391,** 85–100.
36. Diaz, F., Wallner, M., Stefani, E., Toro, L. & Latorre, R. (1996) *J. Gen. Physiol.* **107,** 399–407.
37. Yang, X. C. & Sachs, F. (1989) *Science* **243,** 1068–1071.
38. Ferguson, W. B. (1991) *J. Gen. Physiol.* **98,** 163–181.
39. Shen, K. Z., Lagrutta, A., Davies, N. W., Standen, N. B., Adelman, J. P. & North, R. A. (1994) *Pflügers Arch.* **426,** 440–445.
40. Schreiber, M., Wei, A., Yuan, A., Gaut, J., Saito, M. & Salkoff, L. (1998) *J. Biol. Chem.* **273,** 3509–3516.
41. Moss, B. L. & Magleby, K. L. (2001) *J. Gen. Physiol.* **118,** 711–734.
42. Yuan, A., Dourado, M., Butler, A., Walton, N., Wei, A. & Salkoff, L. (2000) *Nat. Neurosci.* **3,** 771–779.
43. Hille, B., Woodhull, A. M. & Shapiro, B. I. (1975) *Philos. Trans. R. Soc. London B* **270,** 301–318.
44. Islas, L. D. & Sigworth, F. J. (1999) *J. Gen. Physiol.* **114,** 723–742.
45. Blatz, A. L. & Magleby, K. L. (1984) *J. Gen. Physiol.* **84,** 1–23.
46. Eisenman, G., Latorre, R. & Miller, C. (1986) *Biophys. J.* **50,** 1025–1034.
47. MacKinnon, R., Cohen, S. L., Kuo, A., Lee, A. & Chait, B. T. (1998) *Science* **280,** 106–109.
48. Zhou, Y., Morais-Cabral, J. H., Kaufman, A. & MacKinnon, R. (2001) *Nature* **414,** 43–48.